

# What positioning accuracy is sufficient for reliable mmWave A2G channel measurements?

Vasilii Semkin\*, Aki Karttunen<sup>†</sup>, Seongjoon Kang<sup>‡</sup>, Jukka Talvitie<sup>†</sup>, Marco Mezzavilla<sup>‡</sup>,  
Sundeep Rangan<sup>‡</sup>, Mikko Valkama<sup>†</sup>

\*VTT Technical Research Centre of Finland, (*vasilii.semkin@vtt.fi*)

<sup>†</sup>Electrical Engineering Unit, Tampere University, Tampere, Finland, (*firstname.lastname@tuni.fi*)

<sup>‡</sup> NYU Tandon School of Engineering, Brooklyn, NY, USA

**Abstract**—In this work, we investigate the significance of position accuracy for unmanned aerial vehicle (UAV) during millimeter-wave (mmWave) channel measurements. The studies are performed at 28 and 60 GHz frequencies. First, we study the effect of the error in the link distances on the 3GPP channel models. Second, we present ray tracing simulations performed in urban environment. We verify that the horizontal/vertical accuracy of  $\pm 0.5/0.8$  meters may be enough to get reliable data. It should be noted that better accuracy can still improve the results but will require more effort to achieve. In addition, it is confirmed that more severe effect will be visible on the path loss values, while other parameters are not affected as strongly for the LOS case. We present the root mean square error for different positioning accuracies with respect to the reference case, i.e. no error in the UAV position, in angular and time domains which increases linearly with the decreasing accuracy.

**Index Terms**—positioning accuracy, antennas, radio wave propagation, UAV, channel modeling.

## I. INTRODUCTION

Nowadays, UAVs represent a new form factor and are widely utilized by industry and the academy in many areas and applications [1], [2]. It is profoundly improving the services and explicitly provides benefits for future wireless communication systems [3]. For example, UAVs can act as a base station and provide seamless connection to the users or even assist self driving cars and first responders by sharing real time data about the situation on the road. In order to deploy UAV-assisted wireless communications, there is a need in robust channel models required for the wireless system design. There is a growing interest in the air-to-ground (A2G) channel measurements [4], [5] and developing relevant channel models. Most of the studies are focused on sub-6 GHz frequency bands [6], [7], and several target to evaluate the mmWave channel performance, e.g. [8], [9]. It should be noted that A2G channels differ from well-studied terrestrial ones and require careful analysis. The A2G propagation has higher probability for LOS communication, however, the shadowing of the nearby buildings may be present and affect the radio link [3]. For example, authors in [10] highlight height dependent models and mention the necessity for the interference studies. In [11], the coverage in urban environments for the mmWave connectivity to UAVs is presented.

The empirical characterization of the A2G channel is a demanding task due to weight and size constraints for the

payload. Moreover, several issues should be thoroughly considered while planning channel measurements with the UAV-based measurement system. The issues, mentioned in [8], i.e., positioning accuracy, effect of the UAV frame on the antenna pattern, orientation of the UAV, and wobbling effect, may affect the results. In addition, fully coherent measurements may be difficult to obtain due to non-stationary nature of the received signal. In [12], the authors study how the location uncertainty affects channel path loss parameters and study the employment of different channel prediction tools. In [13], similar study is performed for cellular networks. In [14], the authors estimate the impact of positioning accuracy on the path loss model, using smart phones at 2.4 GHz and verify possible correction algorithms. In [15], the authors study wobbling effect of the UAV frame on the channel performance.

In this work, we are going to focus on the following question: *what accuracy is acceptable for radio channel measurements?* and try to find out what is the quantitative characteristic of the acceptable UAV positioning accuracy for radio channel measurements. The results can help to understand positioning error effect and take it into account during planning future measurement campaigns. We are going to focus on mmWave frequency bands, i.e. 28<sup>1</sup> and 60 GHz.

## II. MOTIVATION

Let us first consider possible sources of measurement errors in A2G measurement scenario. (I) The arbitrary orientation of the antenna during the measurements, which is one the possible errors, can be corrected by utilizing a 3-axis gimbal which will stabilize the antenna and allow setting the antenna orientation independently of the UAV orientation. (II) Wobbling effect [15] can be compensated by the gimbal, as well, however, micro-vibrations of the gimbal motors may still affect the results, especially at very high frequencies. This case may require a separate study and is not within the scope of this work. (III) The effect of the UAV hull on the antenna pattern can be significant and should be estimated by antenna measurements or simulations. In Fig. 1, we estimate the effect of the UAV on the omnidirectional antenna located on the bottom of the UAV. One possible way to eliminate this effect is to utilize directional

<sup>1</sup>Formally, 28 GHz frequency is not part of the mmWave band (30 GHz to 300 GHz), however, it is typically considered belonging to mmWave.

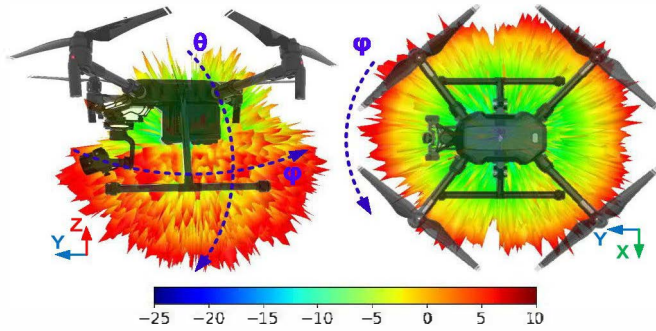


Fig. 1: The effect of the drone frame on the omnidirectional antenna gain pattern. Left - side view, right - view from above.

antennas on the UAV. However, this makes the measurement more complex, since the antenna should be pointed to different directions while UAV is hovering at the point of interest. This approach was used in [9]. This procedure reduces the area covered by the UAV during single flight since UAV has to hover at each position for certain period of time while the measurements are performed for all directions. Another way is to utilize beam steering antenna arrays. However, the effect of the UAV hull may still be present, especially when considering extreme scanning angles. This approach will be considered and studied in the future. Aerial channel measurements with omnidirectional antenna pattern is another approach, which may be suitable when longer flights are performed. (IV) The position of the UAV is usually recorded by the on-board GPS receiver. The accuracy of the GPS receiver is usually in the range of several meters. For example, the best consumer GPS receivers can achieve horizontal and vertical accuracy in urban environments in order of 3 meters and 5.4 meters, respectively [16], however, in dense urban environment the error can be larger. It is necessary to note, that changes in the antenna patterns along with the inaccurate trajectory recording may lead to error in amplitude, delay, or angle of arrival of the received signal). The influence of the positioning error on channel properties, including the antenna patterns effects, are examined by ray-tracing simulations in Sec. IV.

The recorded GPS trajectories for two different GPS receivers, located on the UAV, are presented in Fig. 2. The flights are performed according to the planned way point mission. The routes are compared with respect to each other and to the planned one. It can be noted, that there is a difference in the recordings obtained during different flights by the same GPS receiver, i.e. device 2. The combination of the GPS/GLONASS or GPS/Galileo does not improve the situation (device 1). The real time kinematic (RTK) system may improve the positioning accuracy. However, the question which we are going to tackle in this work: *do we really need high accuracy and what accuracy is sufficient for reliable channel characterization?*

### III. 3GPP PATH LOSS MODEL

The positioning uncertainty in channel measurements cause errors to the link distance estimates, and therefore, errors to link distance dependent channel models. The effect of link distance

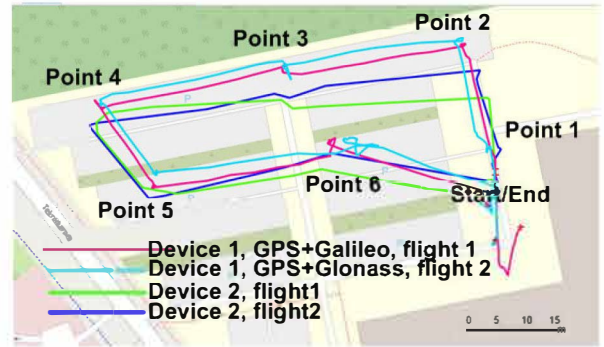


Fig. 2: Comparison between the recorded GPS coordinates by two GPS receivers mounted on the UAV.

error is examined using 3GPP PL-model [17]. In this section, we assume that the positioning uncertainty causes errors only in the link distance in order to get rough estimates for the requirement for the positioning accuracy in different scenarios.

Link distance errors are assumed to be normal distributed

$$d_{\text{error}} = |d + N(0, \sigma_d^2)|, \quad (1)$$

where  $\sigma_d$  is the error standard deviation. Also, to ensure  $\log_{10}(d/d_0) \geq 0$  link distances  $d_{\text{error}} < 1$  m are rounded up to 1 m.

The path loss model is a single slope log-distance model

$$PL(d) = 10 \cdot \alpha \cdot \log_{10}(d/d_0) + \beta + SF, \quad (2)$$

where  $\alpha$  is the path loss exponent,  $\beta$  is the floating point intercept,  $SF$  is the zero-mean shadow fading with variance  $\sigma^2$ , and  $d_0=1$  m is a reference distance. Logarithmic delay spread  $\log_{10}(DS/1s)$  is modeled as a normal distribution with mean  $\mu_{\text{lgDS}}$  and standard deviation  $\sigma_{\text{lgDS}}$ . These parameters are not link distance dependent but the cross-correlation between DS and SF,  $\rho$ , does depend on the link distance dependent path loss model. Note that all cross-correlations between SF and other large scale parameters and SF auto-correlation distance are also affected by link distance errors.

Two example scenarios are examined:

- 1) Urban micro cellular (UMi) scenario in LOS at 60 GHz with link distances from 2 m to 20 m or 2 m to 60 m.
- 2) UMi scenario at 28 GHz with link distances from 10 m to 200 m or 10 m to 600 m. The LOS-state is determined based on the LOS probability model [17].

Path loss and delay spread parameters are given in Table I. Note that the original 3GPP PL models are dual-slope models but the parameters are given for distance under the break point  $d < d_{\text{BP}}$  since the largest link distances  $d_{\text{max}}$  are under the break point at these frequencies.

The PL and DS models, with parameters in Table I, are used to create a large number of PL, SF, and DS values at link distances  $d$ . Then, link distance errors are introduced and the parameters  $\alpha$ ,  $\beta$ ,  $\sigma$ , and  $\rho$  are estimated with the erroneous link distances  $d_{\text{error}}$ . The relative errors in the parameters as a function of the error standard deviation  $\sigma_d$  is presented in

TABLE I: Path loss and delay spread parameters [17].

scenario		UMi		UMi	
		LOS	LOS	NLOS	NLOS
f [GHz]		60		28	
Path loss $d < d_{BP}$	$\alpha$	2.1	2.1	3.53	
	$\beta$	68.0	61.3	53.1	
	$\sigma$	4	4	7.82	
Delay spread	$\mu_{1gDS}$	-7.57	-7.49	-7.18	
	$\sigma_{1gDS}$	0.38	0.38	0.51	
Cross correlation DS vs. SF	$\rho$	-0.4	-0.4	-0.7	

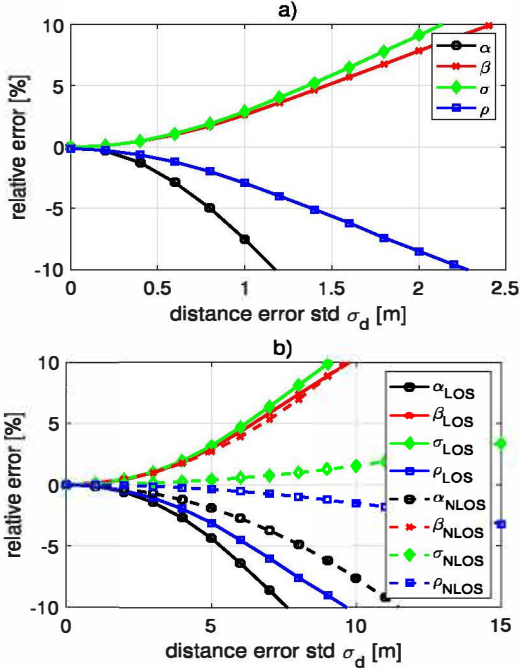


Fig. 3: Relative errors as a function of the link distance error  $\sigma_d$  in a) short range ( $d_{max} = 20$  m) and b) long range ( $d_{max} = 600$  m) examples.

Fig. 3. The errors cause the  $\alpha$  and  $\rho$  to be underestimated and the  $\beta$  and  $\sigma$  to be over estimated.

These results show that the required positioning accuracy for channel measurements depends strongly on the relevant link distance range. The requirement for maximum 10% relative error to the model parameters correspond to maximum 8 m and 15 m distance error standard deviation for  $d_{max} = 200$  m and 600 m, respectively. The corresponding requirement for the 60 GHz LOS case is under 1.2 m and 3.2 m for  $d_{max} = 20$  m and 60 m, respectively. This kind of fairly simple calculations can be used to estimate the needed positioning accuracy before a real measurement campaign.

#### IV. RAY TRACING SIMULATIONS

In order to confirm findings in the previous section, we perform ray tracing simulations in a real scenario where the measurement campaign is planned to be carried out.

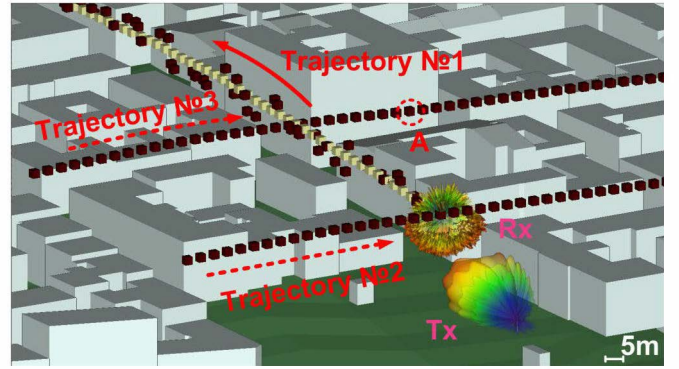


Fig. 4: 3D representation of Helsinki downtown utilized in the ray tracing simulations.

TABLE II: Studied positioning errors for three trajectories.

Name	Horizontal accuracy	Vertical accuracy
Reference case	0	0
Case N <sup>o</sup> 1	$\pm 2$ m	$\pm 3.4$ m
Case N <sup>o</sup> 2	$\pm 1$ m	$\pm 1.7$ m
Case N <sup>o</sup> 3	$\pm 0.5$ m	$\pm 0.8$ m
Case N <sup>o</sup> 4	$\pm 0.1$ m	$\pm 0.17$ m

#### A. Simulation methodology

In this work, we utilize: i) the XGtd software for studying the effect of the UAV frame on the antenna radiation pattern and ii) Wireless InSite for shooting and bouncing ray (SBR) simulations, both provided by Remcom. The UAV model utilized in the simulations is a 3D laser scanned real DJI M210 RTK quadcopter, planned to be used in the future measurement campaigns. An omnidirectional antenna pattern with the gain of 2 dBi is considered for installation on the UAV. The receiving antenna is located on the bottom of the UAV and the resulting radiation pattern is presented in Fig. 1. The UAV frame is made of carbon fiber, with electromagnetic properties similar to perfect electric conductor (PEC), resulting in the antenna gain enhancement and gain fluctuations in certain directions. The positioning error of the UAV of several meters will result in different gain values (e.g., we refer to the XY-plane in Fig. 1) which will affect the received power of the captured rays.

Next, we utilize a simple 3D model of Helsinki city center, Finland, imported to Wireless Insite. The building materials are set to concrete with  $\epsilon_r$  equal to 15. The ray spacing is set to  $0.25^\circ$  and 4 reflections, and 1 diffraction are considered. Horn antenna with the gain of 16 dBi is utilized at the transmitter side and fixed on the ground. We consider three trajectories, as shown in Fig. 4. The height of the UAV is set to 20 meters above the ground level (UAV follows the terrain profile), while the transmitter height is 4 meters. The Tx antenna is tilted upwards by  $15^\circ$ . The simulations are performed in the locations, where planned measurement campaign will take place. In order to introduce the positioning error, we create several routes along the planned trajectories with different positioning accuracy. We study five cases for each trajectory: reference case, which is our planned route, and four cases

with different horizontal and vertical accuracy, summarized in Table II. Generally, we assume that the vertical accuracy is 1.7 times larger than the horizontal one. For each trajectory, we simulate approximately 80 positions of the UAV which are randomly and independently distributed in the defined accuracy limits with uniform distribution. For example, reference cases for all trajectories and case N<sup>o</sup>1 for trajectory N<sup>o</sup>1 are shown in Fig. 4.

### B. Simulation results

We are considering the following parameters in the ray tracing simulations: free space path loss (FSPL) for line of sight (LOS) taking into account antenna radiation patterns, path loss (PL), delay spread (DS) and power angular delay profiles (PADP). In Fig. 5, the FSPL with the antenna patterns is presented. The standard deviation of the FSPL from the reference case for the different positioning errors is shown in Fig. 5, b. It is obvious that increasing positioning accuracy reduces the standard deviation from the reference case. However, it should be noted that case 3 (horizontal error of  $\pm 0.5$ m) and case 4 (horizontal error of  $\pm 0.1$  m) are not very different. Naturally, higher accuracy will be close to the reference route, but the dependence of the positioning accuracy and the obtained FSPL values is not linear, as illustrated in Fig. 5, c. Reducing the error gives better matching with reference case, but, based on these results, it is not necessary to go for higher accuracy than studied in case 3 in case of PL measurements. Almost the same conclusions can be done based on Fig. 6. For the simulated PL values, even the case with the lowest positioning error results in high PL fluctuation, for example, at a distance slightly less than 150 m. This could happen due to positioning error resulting that the UAV is located close to one side of the street, therefore, the communication is possible via the reflection and not the LOS path.

Moreover, we estimate the root mean square error (RMSE) for each trajectory and each positioning error case. Since at every position the received powers are discretely spread in angular and delay domain, we aggregate the received powers which are more than the power threshold, -150 dB, and arrive at a certain angular or delay interval. Thus, we obtain the discrete power set corresponding to several angular or delay bins which consists of several intervals. For each position, RMSE errors are computed between the reference case and studied accuracy cases over the whole bins, and for every trajectory, RMSE errors are taken average over all the position. Fig. 7 shows the RMSE errors for different accuracy cases and trajectories with respect to angular and delay regions. It is visible that the highest accuracy of  $\pm 0.1$ m gives an error of 0.5 dB (Fig. 7, (a)). The error is linearly increasing with decreasing accuracy for all trajectories. The error in delay domain is larger than that in angular domain because even a shortest path can lose much power due to small positional change. In particular, we observe the larger error caused by small positional variation for LOS case. Fig. 7, (b), shows that trajectory 1 (LOS case) gives larger error than trajectories 2 and 3 (combination of LOS and NLOS, while most of the flight route is NLOS). Furthermore,

TABLE III: Path loss and delay spread parameters obtained in the RT simulations for trajectory 1, at 28 and 60 GHz.

$f$	Scenario		Trajectory 1	
			Ref	Case1
28 GHz	PL	$\alpha$	1.91	2.01
		$\beta$	48.0	45.6
		$\sigma$	1.23	1.56
	DS	$\mu_{DS}$	$8.51 \times 10^{-9}$	$8.69 \times 10^{-9}$
		$\sigma_{DS}$	$9.43 \times 10^{-9}$	$7.93 \times 10^{-9}$
60 GHz	PL	$\alpha$	1.96	2.08
		$\beta$	56.57	53.74
		$\sigma$	1.64	1.95
	DS	$\mu_{DS}$	$5.02 \times 10^{-9}$	$4.93 \times 10^{-9}$
		$\sigma_{DS}$	$2.68 \times 10^{-9}$	$2.83 \times 10^{-9}$

in LOS case, the measurement errors can be worse because the variation in the antenna pattern toward LOS path is larger in the close distance.

In addition to the provided results, one appealing question is the positioning accuracy effect for increasing frequencies. This analysis will be performed in the future, however, preliminary simulations are presented in Table III for the LOS case at 28 and 60 GHz. Table III summarizes the path loss and delay spread parameters for trajectory 1 for reference case and the largest positioning error, i.e. case 1.

### V. CONCLUSION AND DISCUSSION

In this work, we present the simulation results of the positioning error on A2G radio channel properties. First, we analyze the effect of the link distance error on the 3GPP path loss model. It is revealed, that in order to get maximum error of 10% at 28 GHz, the standard deviation of the link distance error should be below 8 m for link distances up to 200 m.

The results obtained by the ray tracing simulations provide an insight on which accuracy may be acceptable for certain measurement campaigns depending on the requirements. We confirmed that best positioning accuracy will improve the results and minimize the error. However, we discovered that not necessarily the best positioning accuracy is required for PL estimation. We verified, in particular, that the horizontal accuracy of  $\pm 0.5$  m and vertical accuracy of  $\pm 0.8$  m may be sufficient and will provide similar results as the best studied accuracy (i.e. horizontal accuracy of  $\pm 0.1$ m). This positioning accuracy may be targeted in the measurement campaigns if it is not possible to utilize RTK system to achieve higher accuracy.

In addition, the RMSE is analyzed for defined trajectories and accuracies in angular and time domains. If the goal of measurements is obtaining realistic PADP characteristic, then the highest accuracy will provide realistic results.

### ACKNOWLEDGMENT

The work of V. Semkin was supported in part by the Academy of Finland, projects N<sup>o</sup>331810 and N<sup>o</sup>345372.

### REFERENCES

- [1] Business Insider, "Commercial UAV Market Analysis – Industry trends, forecasts and companies," <https://www.businessinsider.com/commercial-uav-market-analysis>, 2020.

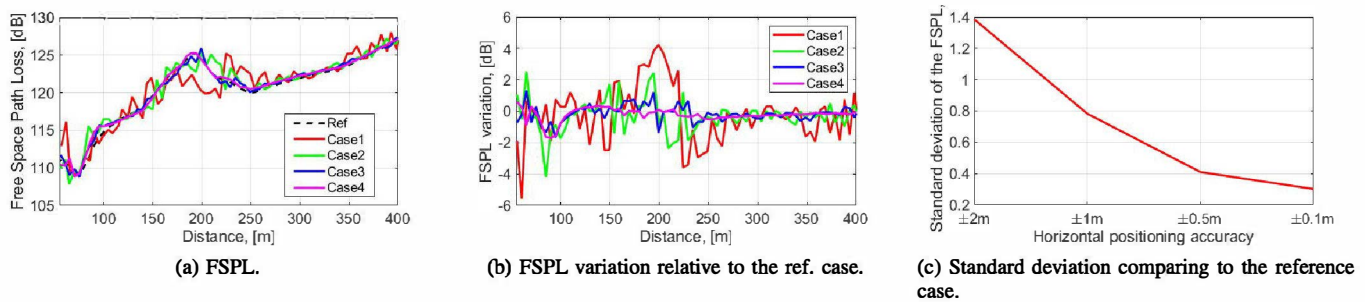


Fig. 5: FSPL for LOS with antenna patterns, trajectory 1 (at 28 GHz). The cases are described in Tab. II.

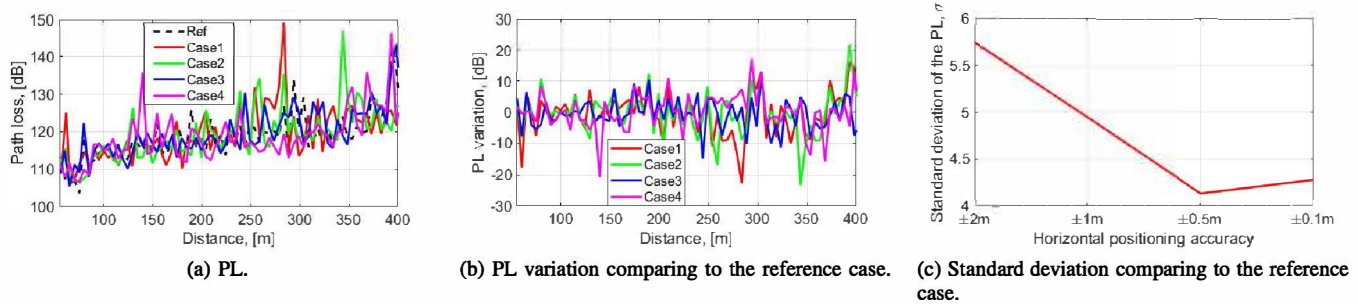


Fig. 6: PL for all positions along the trajectory 1 (at 28 GHz). The cases are described in Tab. II

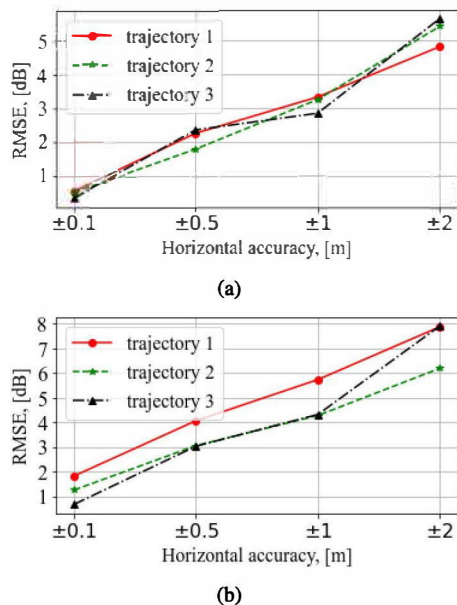


Fig. 7: Comparison of the RMSE with respect to the reference case (at 28GHz) - (a) Angular domain, (b) delay domain.

[2] M. Mozaffari, W. Saad, M. Bennis, Y.-H. Nam, and M. Debbah, "A tutorial on UAVs for wireless networks: Applications, challenges, and open problems," *IEEE Communications Surveys Tutorials*, vol. 21, no. 3, pp. 2334–2360, 2019.

[3] Y. Zeng, I. Guvenc, R. Zhang, G. Geraci, and D. W. Matolak (Eds.), *UAV Communications for 5G and Beyond*. Wiley – IEEE Press, 2020.

[4] A. A. Khuwaja, Y. Chen, N. Zhao, M.-S. Alouini, and P. Dobbins, "A survey of channel modeling for UAV communications," *IEEE Communications Surveys Tutorials*, vol. 20, no. 4, pp. 2804–2821, 2018.

[5] W. Khawaja, I. Guvenc, D. W. Matolak, U. Fiebig, and N. Schneckenburger, "A survey of air-to-ground propagation channel modeling for unmanned aerial vehicles," *IEEE Communications Surveys Tutorials*, vol. 21, no. 3, pp. 2361–2391, 2019.

[6] G. Zhang, X. Cai, W. Fan, and G. F. Pedersen, "A USRP-based channel sounder for UAV communications," in *2020 14th European Conference on Antennas and Propagation (EuCAP)*, 2020, pp. 1–4.

[7] W. Khawaja, I. Guvenc, and D. Matolak, "UWB channel sounding and modeling for UAV Air-to-Ground propagation channels," in *2016 IEEE Global Communications Conference (GLOBECOM)*, 2016, pp. 1–7.

[8] V. Semkin *et al.*, "Lightweight UAV-based measurement system for air-to-ground channels at 28 GHz," in *2021 IEEE 32nd Annual International Symposium on Personal, Indoor and Mobile Radio Communications (PIMRC)*, 2021, pp. 848–853.

[9] E. M. Vitucci *et al.*, "Experimental characterization of air-to-ground propagation at mm-wave frequencies in dense urban environment," in *2021 15th European Conference on Antennas and Propagation (EuCAP)*, 2021.

[10] R. Amorim *et al.*, "Radio channel modeling for uav communication over cellular networks," *IEEE Wireless Communications Letters*, vol. 6, no. 4, pp. 514–517, 2017.

[11] S. Kang *et al.*, "Millimeter-wave UAV coverage in urban environments," available as *arXiv:2104.04600*, 2021.

[12] L. S. Muppirisetty, T. Svensson, and H. Wymeersch, "Spatial wireless channel prediction under location uncertainty," *IEEE Transactions on Wireless Communications*, vol. 15, no. 2, pp. 1031–1044, 2016.

[13] H. Braham, S. B. Jemaa, G. Fort, E. Moulines, and B. Sayrac, "Spatial prediction under location uncertainty in cellular networks," *IEEE Trans. on Wireless Communications*, vol. 15, no. 11, pp. 7633–7643, 2016.

[14] P. M. Santos, T. E. Abrudan, A. Aguiar, and J. Barros, "Impact of position errors on path loss model estimation for device-to-device channels," *IEEE Transactions on Wireless Communications*, vol. 13, no. 5, pp. 2353–2361, 2014.

[15] M. Banagar, H. S. Dhillon, and A. F. Molisch, "Impact of UAV wobbling on the air-to-ground wireless channel," *IEEE Transactions on Vehicular Technology*, vol. 69, no. 11, pp. 14 025–14 030, 2020.

[16] GPS.gov, "GPS Standard Positioning Service (SPS) Performance Standard 5th Edition," 2020.

[17] 3GPP, "Study on channel model for frequencies from 0.5 to 100 GHz," *3GPP TR 38.901 V16.1.0 (2019-12)*.